

M uon-spin-rotation m easurem ents of the penetration depth in $\text{Li}_2\text{Pd}_3\text{B}$

R . K hasanov,^{1,2} C . Baines,² F . La M attina,¹ A . M aisuradze,¹ K . Togano,³ and H . K eller¹

¹Physik-Institut der Universitat Zurich, Winterthurerstrasse 190, CH-8057, Zurich, Switzerland

²Laboratory for M uon Spin Spectroscopy, PSI, CH-5232 Villigen PSI, Switzerland

³National Institute for M aterials Science 1-2-1, Sengen, Ibaraki 305-0047, Japan

M easurem ents of the m agnetic eld penetration depth in the ternary boride superconductor $\text{Li}_2\text{Pd}_3\text{B}$ ($T_c = 7.5\text{ K}$) have been carried out by m eans of m uon-spin-rotation (SR). The absolute values of , the G inzburg-Landau coe cient , and the rst H_{c1} and the second H_{c2} critical eld at $T = 0$ were found to be $(0) = 286(5)\text{ nm}$, $(0) = 31(1)$, $_{0\text{H}}H_{c1}(0) = 7.0(1)\text{ mT}$, and $_{0\text{H}}H_{c2}(0) = 3.58(3)\text{ T}$, respectively. The zero tem perature value of the superconducting gap $_{0\text{H}}$ decreases from $1.35(5)\text{ m eV}$ at $_{0\text{H}} = 0.02\text{ T}$ to $0.56(4)\text{ m eV}$ at $_{0\text{H}} = 2.3\text{ T}$. The ratio $2_{0\text{H}}=k_{\text{B}}T_c$ decreases with increase of m agnetic eld from $4.22(15)$ at $_{0\text{H}} = 0.02\text{ T}$ to $3.69(26)$ at $_{0\text{H}} = 2.3\text{ T}$, implying that the m agnetic eld shifts $\text{Li}_2\text{Pd}_3\text{B}$ superconductor from the strong to the weak coupled regime. At low tem peratures $^2(T)$ saturates and becomes constant below $T = 0.2T_c$, in agreement with what is expected for s-wave BCS superconductors. M easurem ents of the m agnetic eld dependence of reveal that at low tem peratures is alm ost eld independent. Our results suggest that $\text{Li}_2\text{Pd}_3\text{B}$ is a BCS superconductor with an isotropic energy gap.

PACS numbers: 74.70.A d, 74.25.0 p, 74.25.H a, 76.75.+ i, 83.80.F g

I. INTRODUCTION

The discovery of superconductivity in the ternary boride superconductors $\text{Li}_2\text{Pd}_3\text{B}$ and $\text{Li}_2\text{Pt}_3\text{B}$ has attracted considerable interest in the study of these m aterials.^{1,2,3,4,5,7} It is believed now that superconductivity in both above m entioned com pounds is m ost likely m ediated by phonons. It stems from photoem ission,³ nuclear m agnetic resonance (NMR)⁴ and speci c heat⁷ experiments. Moreover, an observation of a Hebel-Schlichter peak in the ^{11}B spin-lattice relaxation rate in $\text{Li}_2\text{Pd}_3\text{B}$ strongly supports singlet pairing.⁴ However, experimental results concerning the structure of the superconducting energy gap are still controversial. On the one hand, NMR⁴ data of $\text{Li}_2\text{Pd}_3\text{B}$ and the speci c heat data of $\text{Li}_2\text{Pd}_3\text{B}$ and $\text{Li}_2\text{Pt}_3\text{B}$ ⁷ can be well explained by assuming presence of the only one isotropic energy gap. On the other hand, m agnetic eld penetration depth m easurem ents suggest the presence of two superconducting isotropic gaps in $\text{Li}_2\text{Pd}_3\text{B}$ and point to the presence of nodes in the gap in $\text{Li}_2\text{Pt}_3\text{B}$.^{5,6} The systematic studies of the m agnetic eld and the tem perature dependences of

can shed light on this discrepancy. In particular, (T) , that re ects the quasiparticle density of states available for thermal excitations, allows to probe the superconducting gap structure. M easurem ents of the eld dependence of allow to study the anisotropy of the superconducting energy gap^{8,9} and, in the case of two-gap superconductors, to obtain information on the relative contribution of each particular gap as a function of m agnetic eld.^{10,11}

In this paper, we report a systematic study of the m agnetic eld and the tem perature dependences of in $\text{Li}_2\text{Pd}_3\text{B}$ by m eans of transverse-eld m uon-spin rotation (TF-SR) (see, e.g., [12]). M easurem ents were performed down to 30 mK in a series of elds ranging from 0.02 T to 2.3 T . For all m agnetic elds studied (0.02 T , 0.1 T , 0.5 T , 1 T , and 2.3 T) the presence of a second superconducting gap has not been detected. Below T_c , the (T) depen-

dences are well tted by assuming presence of the only one isotropic energy gap. The zero-tem perature value of the gap decreases from $1.35(5)\text{ m eV}$ at $_{0\text{H}} = 0.02\text{ T}$ to $0.56(4)\text{ m eV}$ at $_{0\text{H}} = 2.3\text{ T}$. The ratio $2_{0\text{H}}=k_{\text{B}}T_c$ decreases with increase of m agnetic eld from $4.22(15)$ at $_{0\text{H}} = 0.02\text{ T}$ to $3.69(26)$ at $_{0\text{H}} = 2.3\text{ T}$, implying that the m agnetic eld shifts $\text{Li}_2\text{Pd}_3\text{B}$ from a strong-coupled to a weak-coupled superconductor. At low tem peratures the m agnetic penetration depth is alm ost eld independent, in agreement with what is expected for a superconductor with an isotropic energy gap.

The paper is organized as follows: In Sec. II we describe the sample preparation procedure and the TF-SR technique in connection with (T) m easurem ents. Sec. IIIA com prises studies of the tem perature dependence of . In Sec. IIIB results on the m agnetic eld dependence of the zero-tem perature superconducting gap

are reported. In Sec. IIIC we discuss the tem perature dependence of the second critical eld H_{c2} . In Sec. IIID we present the calculation of the absolute value of and its m agnetic eld dependence. The conclusions follow in Sec. IV .

II. EXPERIMENTAL DETAILS

The $\text{Li}_2\text{Pd}_3\text{B}$ alloy sample was prepared by two step arc-m elting.¹ First, a binary Pd_3B alloy was prepared by the conventional arc-m elting from the m ixture of Pd (99.9%) and B (99.5%). The alloying of Li was done in the second arc-m elting, in which a small piece of Pd_3B alloy was placed on a Li (99%) plate. Once the Pd_3B alloy m elted, the reaction with Li occurred and developed very fast, forming a smallbutton specimen (around 300 m g). Since the loss of Li was inevitable, the Li concentration in the nal sample was estimated from the weight change. The deviation of the Li concentration from the stoichiometric one was less than 1% for the specimens used in this experiment.

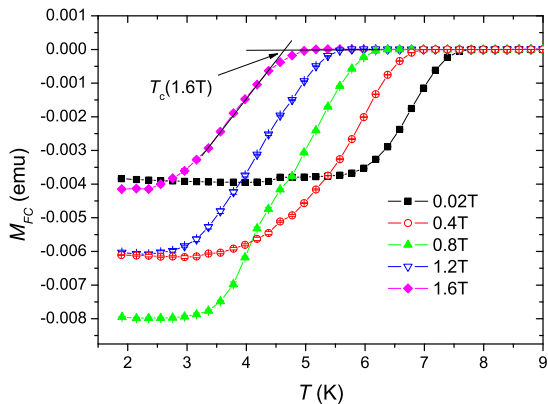


FIG. 1: Field-cooled magnetization $M_{FC}(T)$ of $\text{Li}_2\text{Pd}_3\text{B}$ taken at various magnetic fields: from the left to the right $_{0}\text{H} = 1.6 \text{ T}, 1.2 \text{ T}, 0.8 \text{ T}, 0.4 \text{ T}, \text{ and } 0.02 \text{ T}$. The small paramagnetic background is subtracted.

Field-cooled magnetization (M_{FC}) measurements of $\text{Li}_2\text{Pd}_3\text{B}$ were performed with a SQUID magnetometer in fields ranging from 15 mT to 4 T at temperatures between 1.75 K and 10 K. The transition temperature T_c was obtained as an intersect of the linearly extrapolated $M_{FC}(T)$ curve in the vicinity of T_c with the $M = 0$ line (see Fig. 1).

TF-SR experiments were performed at the M3 beam line at Paul Scherrer Institute (Villigen, Switzerland). The $\text{Li}_2\text{Pd}_3\text{B}$ sample was field cooled from above T_c down to 30 mK in fields of 2.3 T, 1 T and 0.5 T, and down to 1.6 K in fields of 0.1 T and 0.02 T. In the transverse-field geometry the local magnetic field distribution $P(B)$ inside the superconducting sample in the mixed state, probed by means of TF-SR, is determined by the coherence length and the magnetic field penetration depth.

In extreme type II superconductors () $P(B)$ is almost independent on and the second moment of $P(B)$ is simply proportional to $1 = 4^{13}$.

The SR signal was recorded in the usual time-diifferential way by counting positrons from decaying muons as a function of time. The time dependence of the positron rate is given by the expression¹⁴

$$N(t) = N_0 \frac{1}{e} e^{-t} = [1 + aP(t)] + bg; \quad (1)$$

where N_0 is the normalization constant, bg denotes the time-independent background, $= 2.19703(4) \times 10^6 \text{ s}$ is the muon lifetime, a is the maximum decay asymmetry for the particular detector telescope ($a = 0.18$ in our case), and $P(t)$ is the polarization of the muon ensemble:

$$P(t) = \frac{Z}{P(B)} \cos(\theta B t + \phi) dB : \quad (2)$$

Here $= 2 \times 135.5342 \text{ MHz/T}$ is the muon gyromagnetic ratio, and θ is the angle between the initial muon polarization and the effective symmetry axis of a positron

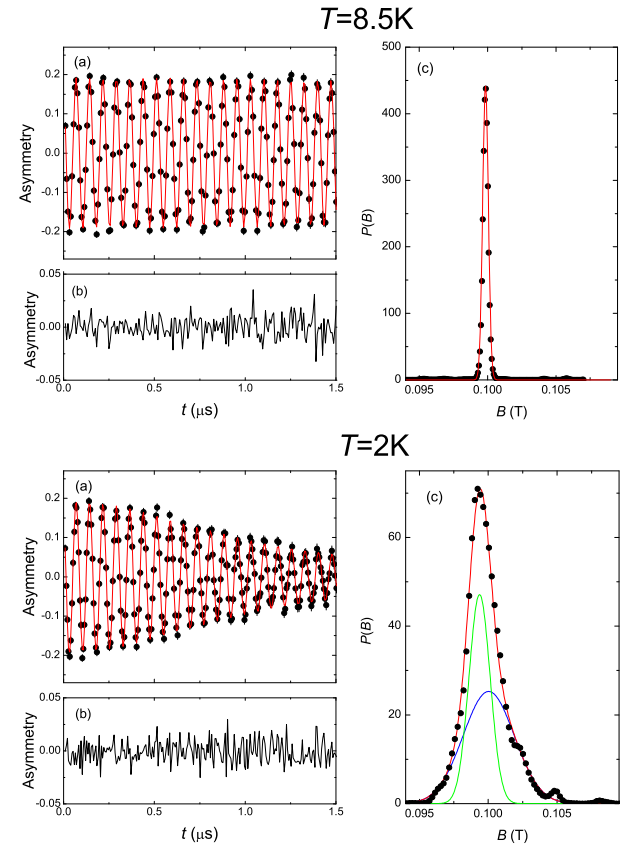


FIG. 2: SR time spectra and magnetic field distributions of $\text{Li}_2\text{Pd}_3\text{B}$ taken above ($T = 8.5 \text{ K}$) and below ($T = 2 \text{ K}$) the superconducting transition temperature T_c at $_{0}\text{H} = 0.1 \text{ T}$: (a) the muon-time spectra, (b) difference between the one Gaussian and two Gaussian fits and experimental data, (c) internal field distributions inside the $\text{Li}_2\text{Pd}_3\text{B}$ sample. The lines represent the best fit with the Gaussian line-shapes. See text for details.

detector. $P(t)$ can be linked to the internal field distribution $P(B)$ by using the algorithm of Fourier transform¹⁴.

The $P(t)$ and $P(B)$ distributions inside the $\text{Li}_2\text{Pd}_3\text{B}$ sample in the normal ($T = 8.5 \text{ K}$) and the superconducting mixed state ($T = 2.0 \text{ K}$) after field-cooling in a magnetic field of 0.1 T are shown in Fig. 2. The $P(B)$ distributions were obtained from the measured $P(t)$ by using the fast Fourier transform procedure based on the maximum entropy algorithm¹⁵. In the normal state, a symmetric line at the position of the external magnetic field with a broadening arising from the nuclear magnetic moments is seen. Below T_c the field distribution is broadened and asymmetric. In order to account for the asymmetric field distribution, SR time spectra obtained below T_c were fitted by two Gaussian lines:^{11,16}

$$P(t) = \sum_{i=1}^{X^2} A_i \exp(-\frac{t^2}{\tau_i^2}) \cos(\theta_i B_i t + \phi_i) : \quad (3)$$

where A_i , τ_i , and B_i are the asymmetry, the Gaussian relaxation rate and the first moment of the i -th line, re-

spectively. At $T > T_c$ the analysis is reduced to a single line with $\omega_{nm} = 0.1$ MHz arising from the nuclear moments of the sample. Eq. (3) is equivalent to the field distribution¹⁶

$$P(B) = \frac{X^2}{i=1} \frac{A_i}{i} \exp \left(-\frac{B_i^2}{2} \right) : \quad (4)$$

The solid lines in Figs. 2 (a) represent the best fit with the one (upper panel) and two Gaussian lines (lower panel) to the SR time spectra. The corresponding $P(B)$ lines are shown in Figs. 2 (c). For this distribution the mean field and the second moment are¹⁶

$$\hbar B_i = \frac{X^2}{i=1} \frac{A_i B_i}{A_1 + A_2} \quad (5)$$

and

$$\hbar B_i^2 = \frac{X^2}{i=1} \frac{A_i^2}{A_1 + A_2} - \frac{1}{2} + B_i \quad \hbar B_i^2 : \quad (6)$$

The superconducting part of the square root of the second moment ($\omega_{sc} / \omega_{nm}^2$) was then obtained by subtracting the nuclear moment contribution (ω_{nm}) measured at $T > T_c$ as $\omega_{sc} = \omega_{nm}^2 - \omega_{nm}^2$. From the known value of ω_{sc} the absolute value of ω_{sc} was calculated from the relation

$$\omega_{sc} [\text{s}^{-1}] = 4.83 \cdot 10^4 (1 - h) [1 + 3.9 (1 - h^2)^{1/2}]^2 [\text{nm}] ; \quad (7)$$

($h = H/H_{c2}$), which describes the field variation in an ideal triangular vortex lattice.¹³

III. EXPERIMENTAL RESULTS AND DISCUSSION

A. Temperature dependence of

In Fig. 3 (a) the temperature dependences of $\omega_{sc} / \omega_{nm}^2$ of $\text{Li}_2\text{Pd}_3\text{B}$ for $H_0 = 0.02$ T, 0.1 T, 0.5 T, 1 T, and 2.3 T are shown. For $H_0 = 0.5, 1$ T, and 2.3 T, $\omega_{sc}(T)$ was measured down to 30 mK. It is seen that below 1.2 K [Fig. 3(b)] $\omega_{sc}^2 / \omega_{nm}^2$ is temperature independent in agreement with what was observed in Ref. [5]. Note that a constant value of $\omega_{sc}^2 / \omega_{nm}^2$ is expected for BCS-type superconductors.¹⁷ The solid lines in Fig. 3 represent fits with the BCS model.¹⁷

$$\frac{\omega^2(T; \omega_0)}{\omega^2(0)} = 1 + 2 \frac{Z_1}{(T)} \frac{\partial f}{\partial E} \frac{E}{E^2 - (T)^2} dE : \quad (8)$$

Here, $f = (1 + \exp(E/k_B T))^{-1}$ is the Fermi function, $Z_1(T) = \omega_0(T/T_c)$ represents the temperature dependence of the energy gap, k_B is the Boltzmann constant, and ω_0 denotes the zero temperature value of the superconducting gap. For the normalized gap $\tilde{\omega}(T=T_c)$ the values tabulated in Ref. [18] were used. The data in the Fig. 3 were fitted with $\omega_{sc}(0)$ and ω_0 as free parameters, and T_c fixed (the values of T_c were extracted from the

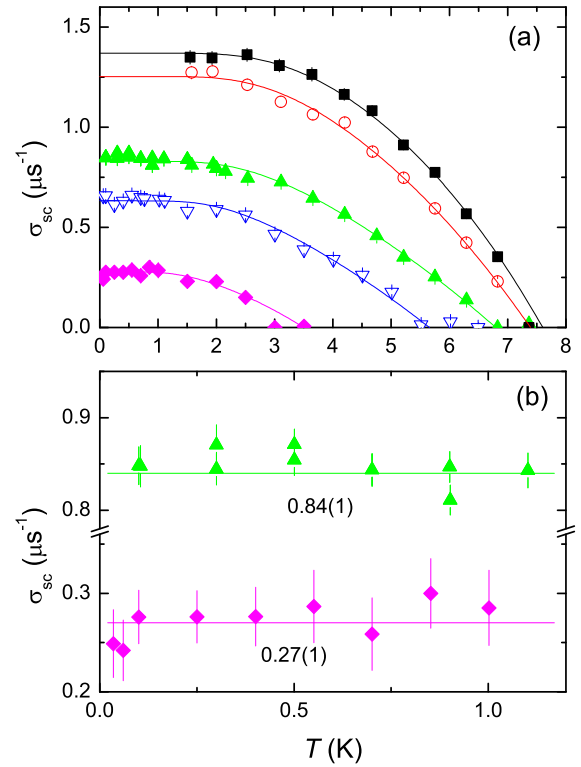


FIG. 3: (a) Temperature dependence of $\omega_{sc} / \omega_{nm}^2$ of $\text{Li}_2\text{Pd}_3\text{B}$ measured in various magnetic fields (from top to the bottom) 0.02 T, 0.1 T, 0.5 T, 1.0 T and 2.3 T. Solid lines represent fits with the weak coupling BCS model.¹⁷ (b) Low-temperature part of $\omega_{sc}(T)$ for $H_0 = 0.5$ T and 2.3 T.

TABLE I: Summary of some physical parameters obtained from the fits of $\omega_{sc}(T)$ data of $\text{Li}_2\text{Pd}_3\text{B}$ (see text for an explanation).

| H_0 (T) | T_c (K) | ω_0 (m eV) | $\omega_{sc}(0)$ (μs^{-1}) |
|--------------|--------------|----------------------|--|
| 0.02 | 7.39(3) | 1.35(5) | 4.22(15) |
| 0.1 | 7.20(3) | 1.21(5) | 3.91(16) |
| 0.5 | 6.51(3) | 1.03(5) | 3.66(18) |
| 1.0 | 5.63(3) | 0.85(5) | 3.51(21) |
| 2.5 | 3.50(3) | 0.56(4) | 3.69(26) |

corresponding field-cooled magnetization measurements, see Fig. 1). The results of this analysis are summarized in Table I.

Recently Yuan et al.⁵ have performed a $\omega_{sc}(T)$ study in $\text{Li}_2\text{Pd}_3\text{B}$ by means of the self-inductance technique. It was found that $\omega_{sc}(T)$ below $T = 2.5$ K cannot be described by a single gap model, and thus the presence of the second superconducting gap was assumed. Our data, however, are well described by a single gap model. The reason for this discrepancy is most probably the follow-

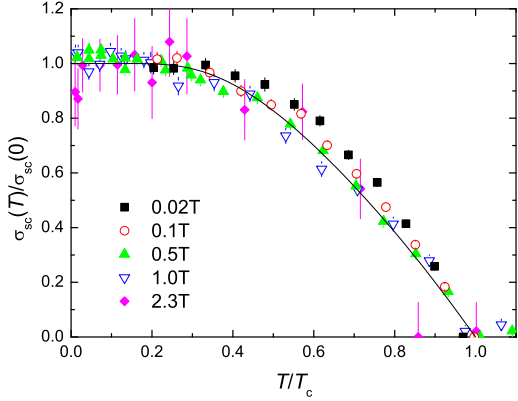


FIG. 4: Normalized superfluid density $\sigma_{sc}^2(T)/\sigma_{sc}^2(0) = \sigma_{sc}(T)/\sigma_{sc}(0)$ versus the reduced temperature $T=T_c$ of $\text{Li}_2\text{Pd}_3\text{B}$ measured in various magnetic fields (0.02 T, 0.1 T, 0.5 T, 1 T, and 2.3 T). The solid line represents a fit of the SR data for 0.5 T with Eq. (8).

ing. The contribution of the smaller gap to the superfluid density is expected to be stronger suppressed by a magnetic field than the bigger one. Such a behavior was recently observed in the double-gap MgB_2 superconductor in magnetization¹⁰ and SR experiments.¹¹ The measurements in Ref. [5] were performed in zero magnetic field, and the contribution of the smaller gap was found to be of the order of 5% only. Thus, even the lowest field in which our experiments were performed (0.02 T), probably leads to an almost complete suppression of the contribution of the smaller gap to the superfluid density, implying that $\text{Li}_2\text{Pd}_3\text{B}$ behaves effectively as a single gap superconductor.

Additional support of single-gap behavior comes from the comparison of the $\sigma(T)$ curves measured in different fields. It was observed that in MgB_2 the suppression of the smaller gap by a magnetic field results in substantial change of the shape of $\sigma(T)$.¹⁹ For this reason in Fig. 4 we plot the normalized superfluid density $\sigma^2(T)/\sigma^2(0) = \sigma_{sc}(T)/\sigma_{sc}(0)$ versus the reduced temperature $T=T_c$ for various magnetic fields. It is seen that all the curves almost collapse to the single line, indicating that $\sigma^2(T)$ measured at different fields is nearly the same.

To summarize, in the whole temperature range (from T_c down to 30 mK) the temperature dependence of σ is consistent with what is expected for a single-gap s-wave BCS superconductor. Moreover, $\sigma(T)$ was found to be almost independent of the magnetic field.

B. Dependence of the zero-temperature superconducting gap Δ_0 on the critical temperature T_c

In Fig. 5 we plot the zero-temperature superconducting gap Δ_0 obtained from the fit of $\sigma^2(T)$, see Table I] as a function of the critical temperature T_c . In addition the values of the bigger superconducting gap $\Delta_0 = 0.995$ m eV obtained by Yuan et al.⁵ and $\Delta_0 = 1.27(4)$ m eV from

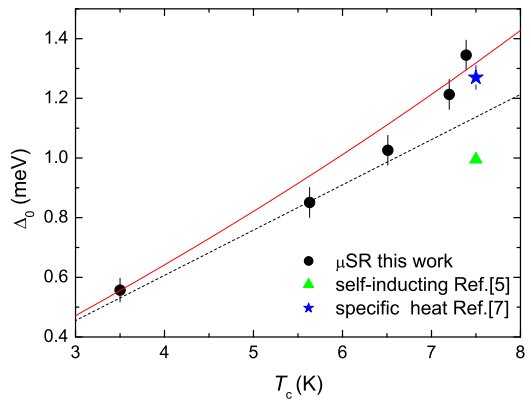


FIG. 5: Zero-temperature superconducting gap Δ_0 as a function of the transition temperature T_c for $\text{Li}_2\text{Pd}_3\text{B}$. For comparison the values of Δ_0 reported in Refs. [5] and [7] are also included. The dashed line represents the universal BCS line with $\Delta_0 = k_B T_c = 3.52$. The solid line is obtained from Eq. (9) with the parameters given in the text.

Ref. [7] are also included on the graph. Note that decrease of the transition temperature T_c is caused by the increase of the external magnetic field. The dashed line represents the universal BCS line with $\Delta_0 = k_B T_c = 3.52$. It is seen that with decreasing T_c the experimental points have the tendency to approach the universal BCS line. In other words, the ratio $\Delta_0/k_B T_c$ decreases with decreasing T_c . Inspection of the Table I reveals that the ratio decreases from 4.22(15) at $T_c = 7.39$ K ($\mu_0 H = 0.02$ T) to 3.69(26) at $T_c = 3.50$ K ($\mu_0 H = 2.3$ T). This means that the coupling strength in $\text{Li}_2\text{Pd}_3\text{B}$ changes with decreasing T_c (increasing magnetic field). At low fields (high T_c) $\text{Li}_2\text{Pd}_3\text{B}$ is a strong coupled BCS superconductor, while at high-fields (low T_c) it becomes weak-coupled. This behavior can be understood in the framework of the theory developed by Mitravic et al.²⁰ which predicts a deviation of the ratio $\Delta_0/k_B T_c$ from the BCS value of 3.52 due to strong-coupling effects:

$$\frac{\Delta_0}{k_B T_c} = 3.53 \cdot 1 + 12.5 \cdot \frac{k_B T_c}{\omega_{\text{ln}}}^2 \ln \frac{\omega_{\text{ln}}}{2k_B T_c} ; \quad (9)$$

where ω_{ln} is a characteristic phonon frequency defined as the logarithmic moment of the electron-phonon spectral function $\text{F}(\omega)$.²¹ Bearing in mind that ω_{ln} does not depend on the magnetic field, Eq. (9) suggests that the ratio $\Delta_0/k_B T_c$ decreases monotonically with decreasing T_c . The solid line in Fig. 5 represents the theoretical $\Delta_0(T_c)$ curve obtained by using Eq. (9) with $\omega_{\text{ln}} = 9.48$ m eV reported in Ref. [7]. Note that Eq. (9) describes the general behavior of $\Delta_0(T_c)$ rather well, but a systematic deviation between experimental theory is obvious. It may be that the phonon spectrum of $\text{Li}_2\text{Pd}_3\text{B}$ cannot be satisfactorily described with a single phonon energy, and thus the traditional Eliashberg electron-phonon coupling equations, that were used to derive Eq. (9),²⁰ are not adequate.

Note that in the isomorphic compound $\text{Li}_2\text{Pt}_3\text{B}$ ($T_c = 2 \text{ K}$), the ratio $2 \frac{1}{k_B} T_c = 3.53$ was found to be very close to the weak-coupled BCS value 3.52 (see Ref. [7]). It is remarkable that in $\text{Li}_2\text{Pd}_3\text{B}$ the ratio $2 \frac{1}{k_B} T_c$ has the tendency to reach this value when T_c decreases. The authors in Ref. [7] suggest that the rather different values of T_c of the two isomorphic compounds $\text{Li}_2\text{Pd}_3\text{B}$ ($T_c = 7.5 \text{ K}$) and $\text{Li}_2\text{Pt}_3\text{B}$ ($T_c = 2 \text{ K}$) is probably due to the smaller value of the quantity $hI^2i = h!^2i$ in the latter compound. Here, hI^2i is the squared electron-phonon matrix element, and $h!^2i$ is the average of the squared phonon frequency over the Fermi surface. They were not able, however, to distinguish which particular term (hI^2i or $h!^2i$) is responsible for the decrease of the coupling strengths in these materials. Bearing in mind that with decreasing T_c the ratio $2 \frac{1}{k_B} T_c$ in $\text{Li}_2\text{Pd}_3\text{B}$ tends to the same value as in $\text{Li}_2\text{Pt}_3\text{B}$, and assuming that the magnetic field should not affect the phonon spectra, we can argue that hI^2i is mainly responsible for the change in the coupling strength.

C. Temperature dependence of the second critical field

In order to extract the absolute value of the penetration depth from the SR depolarization rate σ_{sc} one needs to know the zero-temperature value of the second critical field H_{c2} [see Eq. (7)]. $H_{c2}(T)$ was obtained from the field-cooled magnetization curves [$M_{FC}(T; H = \text{const})$] measured in constant magnetic fields, ranging from 15 mT to 4 T (see Fig. 6). For each particular field H the corresponding $T_c(H)$ was taken as the temperature where $H = H_{c2}(T = T_c)$ (see Fig. 1).

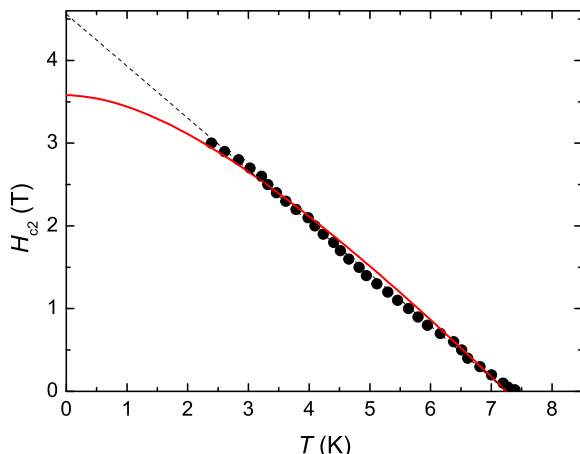


FIG. 6: Temperature dependence of the second critical field H_{c2} of $\text{Li}_2\text{Pd}_3\text{B}$ obtained from $M_{FC}(T)$ measurements (see text for an explanation). The solid and the dotted lines are the linear fit and the fit by means of the W HH model to $H_{c2}(T)$ data. The fit parameters are listed in the text.

The second critical field of a superconductor is determined by the combined effects of an external magnetic field on the spin and the orbital degrees of freedom of the conduction electrons. Werthammer et al.²² worked out a theory (W HH theory) for H_{c2} which includes both spin and orbital paramagnetic effects. For BCS superconductors in the dirty limit ($\lambda = l, l$ is the mean free path) the W HH theory reveals:

$$\ln \frac{1}{t} = \sum_{n=1}^{\infty} \frac{1}{2n+1j} \frac{2n+1j + \frac{\tilde{h}}{t}}{+ \frac{(\frac{M}{B} \tilde{h} = t)^2}{2n+1j + (\tilde{h} + \frac{so}{B}) = t}} ; \quad (10)$$

where $\tilde{h} = h = 0.281$ is the W HH reduced field, $t = T = T_c(H = 0)$ denotes the reduced temperature and $\frac{M}{B}$ and $\frac{so}{B}$ are the Maki²³ and the W HH spin-orbit parameters, respectively. The Maki parameter is related to the slope of $H_{c2}(T)$ in the vicinity of T_c and the value of the superconducting gap Δ_0 in the following manner²³

$$\frac{M}{B} = 0.693 \frac{(dH_{c2}/dT)_{T=T_c}}{H_P} = 0.693 \frac{(dH_{c2}/dT)_{T=T_c}}{0(H=0)} ; \quad (11)$$

where $\frac{B}{B}$ is the Bohr magneton and H_P is the Pauli paramagnetic limiting field. Following Clogston,²⁴ H_P can be obtained as $H_P = \Delta_0(H=0) = \frac{2}{3} \frac{B}{B}$. The linear fit of $H_{c2}(T)$ data yields $dH_{c2}/dT = -0.63 \text{ T/K}$. By substituting this and $\Delta_0(0.02 \text{ T}) = 1.37(5) \text{ meV}$ (see Table I) to the Eq. (11) the value of the Maki parameter is found to be $\frac{M}{B} = 0.34(4)$. Applying now Eq. (10) to the experimental $H_{c2}(T)$ data we get $T_{c0} = 7.32 \text{ K}$, $\Delta_0(H_{c2}(0)) = 3.58(3) \text{ T}$ (solid line in Fig. 6). Note that, the fit of Eq. (10) to the experimental data is statistically correct for all $\frac{so}{B}$ higher than 6. The high value of $\frac{so}{B}$ together with small value of $\frac{M}{B}$ implies that in $\text{Li}_2\text{Pd}_3\text{B}$ the spin-orbital effects play an important role for superconductivity.

D. The zero temperature value of

Within BCS theory the zero-temperature magnetic penetration depth of an isotropic superconductor does not depend on the value of the magnetic field. On the other hand, in superconductors with nodes in the gap and isotropic double-gap superconductors like MgB_2 ($T_c = 39 \text{ K}$) is expected to increase with increasing magnetic field (see e.g., Refs. [8,9,11]). In order to distinguish between the two-gap scenario proposed in Ref. [5] and the single-gap scenario suggested in the present study we performed an analysis of the magnetic field dependence of the zero-temperature muon depolarization rate $\sigma_{sc}(0)$ (see Table I). $\sigma_{sc}(0)$ decreases from 1.37 s^{-1} to 0.28 s^{-1} with magnetic field increasing from 0.02 T to 2.3 T (see Fig. 7). Fitting of Eq. (7) with $\Delta_0(0)$ as free parameter and $H_{c2}(0) = 3.58(3) \text{ T}$ (see sec. IIIC) to the experimental data yields $\Delta_0(0) = 286(5) \text{ nm}$. The agreement between theory and experimental data is rather good.

In the next step we performed a fit assuming that (0) changes linearly with field³

$$(0;h) = (0;0)(1 + h): \quad (12)$$

The fit reveals (0) = 282(7) nm and = 0.18(21). Kadono⁸, has shown that the linear coefficient lies in a range of 1 to 6 for unconventional superconductors (including double-gap MgB₂), while '0' for superconductors with an isotropic energy gap. Thus the observation of an almost zero (within error) confirms that Li₂Pd₃B has an isotropic energy gap.

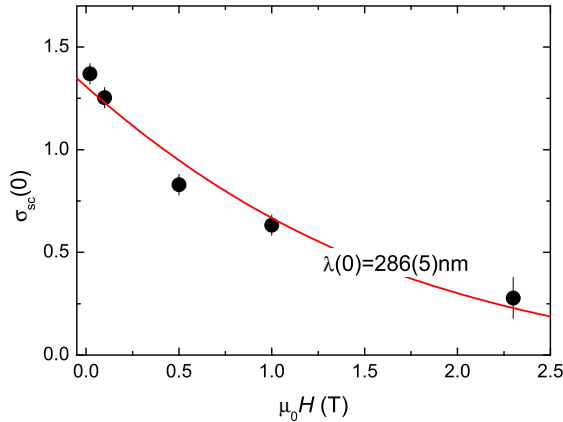


FIG. 7: Field dependence of the zero-temperature SR depolarization rate $\sigma_0(0)$ in Li₂Pd₃B sample. The solid line corresponds to a fit of Eq. (7) to the experimental data with the parameters given in the text.

The value of the first critical field H_{c1} was estimated from the Ginzburg-Landau equation $H_{c1}(0) = \frac{1}{2} \ln \left(\frac{2}{\lambda} \right)$ (0) (0 is the magnetic flux quantum, $\lambda = \frac{e}{2\pi} \frac{1}{k_B T_c}$ is the Ginzburg-Landau parameter, and λ_{GL} is the Ginzburg-Landau coherence length). Using the measured value (0) = 286(5) nm and $\lambda_{GL}(0) = 9.1$ nm taken from Ref. [2], we find $\lambda(0) = 7.0(1)$ mT and $\lambda = 31(1)$. Note that our value of $H_{c1}(0)$ is almost a factor of two smaller than the value $\lambda(0) = 13.5$ mT reported by Badica et al.² In Ref. [2] H_{c1} was defined as the point where the magnetization curves M(H) start to deviate from the straight line. In this case the estimate

of H_{c1} highly depends on the criteria used to account for such a deviation, and consequently the absolute value of H_{c1} can be overestimated.

To summarize, the absolute value of the zero-temperature penetration depth was found to be (0) = 286(5) nm. The first critical field and the Ginzburg-Landau coefficient were estimated to be $H_{c1}(0) = 7.0(1)$ mT and (0) = 31(1), respectively. (0) was found to be field independent, suggesting that the superconducting energy gap in Li₂Pd₃B is isotropic.

IV. CONCLUSIONS

Muon-spin rotation and magnetization studies were performed on the ternary boride superconductor Li₂Pd₃B ($T_c = 7.5$ K). The main conclusions are: (i) The absolute values of $\sigma_0(0)$, $H_{c1}(0)$, and $H_{c2}(0)$ at zero temperature obtained from SR and magnetization experiments are: (0) = 286(5) nm, (0) = 31(1), $\lambda(0) = 7.0(1)$ mT, and $\lambda_{GL}(0) = 9.1(1)$ nm. (ii) Over the whole temperature range (from T_c down to 30 mK) the temperature dependence of $\sigma_0(T)$ is consistent with what is expected for a single-gap s-wave BCS superconductor. (iii) The shape of $M(T)$ is almost independent of the magnetic field. (iv) The ratio $2\lambda = k_B T_c$ decreases with decreasing T_c (increasing magnetic field) from 4.22(15) at $T_c = 7.39$ K ($\lambda(0) = 0.02$ T) to 3.69(26) at $T_c = 3.50$ K ($\lambda(0) = 2.3$ T), implying that the magnetic field shifts Li₂Pd₃B superconductor from a strong-coupled to a weak-coupled regime. (v) At $T = 0$ the magnetic penetration depth is almost field independent, in agreement with what is expected for a superconductor with an isotropic energy gap. (vii) The initial slope of H_{c2} is -0.63 T/K, corresponding to a Meissner parameter $M = 0.34(4)$.

To conclude, all the above mentioned features suggest that Li₂Pd₃B is a BCS superconductor with an isotropic energy gap.

V. ACKNOWLEDGMENTS

This work was partly performed at the Swiss Muon Source (SMS), Paul Scherrer Institute (PSI, Switzerland). The authors are grateful to M. Belogolovski for helpful discussions and S. Strassle for help during manuscript preparation. This work was supported by the Swiss National Science Foundation.

¹ K. Togano, P. Badica, Y. Nakamori, S. Orimo, H. Takeya, and K. Hirata, Phys. Rev. Lett. 93, 247004 (2004).

² P. Badica, T. Kondo, T. Kudo, Y. Nakamori, S. Orimo, and K. Togano, Appl. Phys. Lett. 85, 4433 (2004).

³ T. Yokoya, T. Muro, I. Hase, H. Takeya, K. Hirata, and K. Togano, Phys. Rev. B 71, 092507 (2005).

⁴ M. Nishiyama, Y. Inada, and Guo-qing Zheng, Phys. Rev. B 71, 220505(R) (2005).

⁵ H. Q. Yuan, D. Vandervelde, M. B. Salamon, P. Badica, and

K. Togano, cond-mat/0506771 (unpublished).

⁶ H. Q. Yuan, D. F. Agterberg, N. Hayashi, P. Badica, D. Vandervelde, K. Togano, M. Sigrist, M. B. Salamon, cond-mat/0512601 (unpublished).

⁷ H. Takeya, K. Hirata, K. Yamada, K. Togano, M. El-Maslamani, R. Rapp, F. A. Chaves, and B. Ouladdiaf, Phys. Rev. B 72, 104506 (2005).

⁸ R. Kadono, J. Phys.: Cond. Mat. 16, S4421 (2004).

⁹ J. Sonier, J. Brewer, and R. Kie, Rev. Mod. Phys. 72,

769 (2000).

¹⁰ M . Angst, D D i Castro, D G . Eshchenko, R . K hasanov, S . Kohout, I M . Savic, A . Shengelaya, S L . Bud'ko, P C . Can old, J . Jun, J . Karpinski, S M . Kazakov, R A . Ribeiro, and H . Keller, Phys. Rev. B 70, 224513 (2004).

¹¹ S . Serventi, G . A lodi, R D e Renzi, G . Guidi, L . Rom an, P . M anfrinetti, A . Palenzona, Ch . Niederm ayer, A . Am ato, and Ch . Baines, Phys. Rev. Lett. 93, 217003 (2004).

¹² P . Zim mern, H . Keller, S . L . Lee, I . M . Savic, M . W arden, D . Zech, R . Cubitt, E . M . Forgan, E . Kaldis, J . Karpinski, and C . K ruger, Phys. Rev. B 52, 541 (1995).

¹³ E H . B randt, Phys. Rev. B 37, 2349 (1988).

¹⁴ A . Schenck, Mu on Spin Rotation: Principles and Applications in Solid State Physics, (Adam H ilger, Bristol, 1986); S F J . Cox, J . Phys. C 20, 3187 (1987); J H . B rauer, "Mu on Spin Rotation/Relaxation/Resonance" in Encyclopedia of Applied Physics Vol. 11, p. 23 (VCH, New York, 1995).

¹⁵ B D . Rainford and G J . Daniell, Hyper ne Interact. 87, 1129 (1994).

¹⁶ R . K hasanov, D G . Eshchenko, D D i Castro, A . Shengelaya, F La M attina, A . M aisuradze, C . Baines, H . Luetkens, J . Karpinski, S M . Kazakov, and H . Keller, Phys. Rev. B 72, 104504 (2005).

¹⁷ M . Tinkham, "Introduction to Superconductivity", K rieger Publishing company, M alabar, Florida, 1975.

¹⁸ B . M uhl schlegel, Z . Phys. 155, 313 (1959).

¹⁹ Ch . Niederm ayer, C . Bernhard, T . Holden, R K . K rem er, and K . Ahn, Phys. Rev. B 65, 094512 (2002).

²⁰ B . M itrovic, E . Schachinger, and J P . Carbotte, Phys. Rev. B 29, 6187 (1984).

²¹ P B . Allen and R C . Dynes, Phys. Rev. B 12, 905 (1975).

²² N R . W erthamer, E . H elfand, and P C . H ohenberg, Phys. Rev. 147, 295 (1966).

²³ K . M aki, Phys. Rev. 148, 362-369 (1966).

²⁴ A M . C logston, Phys. Rev. Lett. 15, 266 (1962).